Empirical Wavelet Fractal Texture Analysis for Skin Disease Identification

S. Chatterjee[1], D. Dey[2] and S. Munshi[3]
Department of Electrical Engineering, Jadavpur University
Kolkata, India
[1]saptarshichatterjee2009@gmail.com, [2]debangshudey80@gmail.com
[3]sugatamunshi@yahoo.com

***Abstract*—This research paper reports a methodology for the development of computer aided four class skin disease identification technique. Identification of significant informatics regions from the skin lesion in naked eye examination is very much challenging for the radiologist and expert. This may lead to the improper diagnosis and further prevention of the disease. In this work, dermoscopic image is decomposed into different frequency spectrum by employing empirical wavelet transform to analyze the complex textural properties of the lesion. For the quantitative analysis of textural complexity, empirical wavelet fractal descriptor (EWFD) is introduced. After extracting the morphological, texture and color features, a recursive feature elimination based feature selection technique is used to classify melanoma, nevus, BCC and SK diseases. Employing ensemble multiclass classification strategy, sensitivity of 99.20%, 98.60%, 98.20% and 98.80% is achieved for melanoma, nevus, BCC and SK diseases respectively.**

Keywords— classifier, empirical wavelet transform, recursive feature elimination, skin disease, support vector machine.

I. INTRODUCTION

Development of computer aided diagnostic (CAD) system has a significant contribution on early stage detection and accurate diagnosis of numerous human disorders. Among various types of diseases, skin cancer is considered to be one of the deadliest in all over the world [1]. For thorough investigation and in-depth visualisation, dermatologists use dermoscopy or dermatoscopy, a micro morphological imaging technique [2]. However, the complex structure and closely similar visual appearance make it difficult for the general physicians and experts to make a proper conclusive decision at a very early stage of the diseases. Here, the extensive use of signal processing tools performs a significant role in early and accurate diagnosis of the disease by means of extracting meaningful representative features. Literature suggests various efficient feature extraction tools for the classification of skin abnormalities. Barata *et. al.* have proposed two systems for melanoma identification using global and local textural and color features with 96% sensitivity and 80% specificity [3]. Simizu *et. al.* have introduced a task decomposition based four class classification technique to differentiate melanoma, nevus, BCC and SK skin lesions, with 90.48%, 82.51%, 82.61%, and 80.61% identification rate respectively [4]. Considering the combined feature set of texture, shape and color, melanoma and dysplastic nevi lesions have been differentiated by Rastgoo *et. al.* [5]. Jiji *et al.* have proposed a content based image retrieval technique for the extraction of visual information from the dermoscopic images, and particle swarm optimization technique for multi-class classification of skin lesions [6].

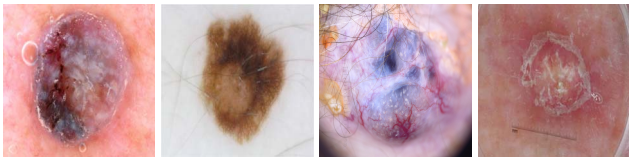

(a) *(b)* *(c)* *(d)*

Fig.1. Sample dermoscopic images, (a) melanoma, (b) nevus, (c) BCC and (d) SK.

In this report work, four varieties of skin diseases as melanoma, nevus, Basal Cell Carcinoma (BCC) and Seborrhoeic Keratosis (SK) have been classified using multi-class classification technique. Example of some sample dermoscopic images of these four disease classes are shown in Fig.1. In this research work, empirical wavelet fractal descriptor (EWFD) is introduced to realise the textural variations and extract the statistical features. Finally, an ensemble multiclass classification model is employed for the identification of four skin disease classes.

This research paper is organised as the following. In section II the theoretical background of empirical wavelet transform (EWT) is discussed. In Section III the detail description of the proposed methodology is given followed by results and discussion in Section IV. This research paper is concluded in Section V.

II. EMPIRICAL WAVELET TRANSFORM: A CURSORY VIEW

Wavelet analysis is one of the most efficient tools for signal and image processing. For multi-resolution analysis, a mother wavelet of varying width with low and high frequency bases is used for detecting the image discontinuities. A particular rigid mother wavelet is used to construct a filter bank for the time-frequency analysis of an image. An adaptive extension is employed in the wavelet packet decomposition technique by successive refinement of the scale. However, a constant ratio in the successive subdivision limits the adaptability [7, 8].

Empirical wavelet transform (EWT) is an adaptive methodology for spatial-spectral analysis of an image to construct wavelet bases directly from the information contained in the image itself. The EWT consists of two major steps: estimation of the Fourier supports followed by construction of corresponding wavelet bases as per those supports. In EWT, considering the Shannon criterion, the normalized Fourier support from 0 to π is segmented into S contiguous segments, $\omega_0 = 0$ to $\omega_S = \pi$. Each segment,

978-1-7281-7366-5/20/$31.00 ©2020 IEEE

centered around ω_s with a transition phase of T_s of width $2\tau_s$. The arbitrary function $\beta(m)$ can defined as [8, 9]:

$$\beta(m)=\begin{cases}0 & if\ m\le 0\\ \quad and\ \beta(m)+\beta(1-m)=1 & \forall m\in[0,1]\\ 1 & if\ m\ge 1\end{cases} \quad (1)$$

Considering τ_s proportional to $\omega_s : \tau_s = \lambda\omega_s$ where $0<\lambda<1$ empirical scaling function $(\xi_m(\omega))$ and the empirical wavelets $(\varsigma_m(\omega))$ are defined as band pass filters and expressed as the following:

$$\xi_m(m)=\begin{cases}1 & if\ |\omega|\le(1-\lambda)\omega_m\\ \cos\left[\frac{\pi}{2}\beta\left(\frac{1}{2\lambda\omega_s}\left(|\omega|-(1-\lambda)\omega_s\right)\right)\right] & \\ \quad if\ (1-\lambda)\omega_s\le|\omega_s|\le(1+\lambda)\omega_s & \\ 0 & otherwise\end{cases} \quad (2)$$

$$\varsigma_m(\omega)=\begin{cases}1 & if\ (1+\lambda)\omega_m\le|\omega|\le(1-\lambda)\omega_m\\ \cos\left[\frac{\pi}{2}\beta\left(\frac{1}{2\lambda\omega_{m+1}}\left(|\omega|-(1-\lambda)\omega_{m+1}\right)\right)\right] & \\ \quad if\ (1-\lambda)\omega_{m+1}\le|\omega|\le(1+\lambda)\omega_{m+1} & \\ \sin\left[\frac{\pi}{2}\beta\left(\frac{1}{2\lambda\omega_m}\left(|\omega|-(1-\lambda)\omega_m\right)\right)\right] & \\ \quad if\ (1-\lambda)\omega_m\le|\omega|\le(1+\lambda)\omega_m & \\ 0 & otherwise\end{cases} \quad (3)$$

In this proposed technique, 2D empirical Littlewood-Paley wavelet transform has been employed to decompose the input image in low and high frequency components. To perform 2D EWT of the image (*I*), 1D Fourier Transform is performed along each row and column of the image to calculate the mean row and column magnitude spectrum. Fourier boundaries have been detected from row and column spectrums to construct the corresponding filter bank. From each of the filter, corresponding sub-band images are obtained.

III. Proposed Methodology

Identification of skin diseases comprises of four basic steps: image pre-processing, segmentation, feature extraction and classification. The contaminating noise introduced from uneven lighting conditions and hair artefacts in the input dermoscopic images are removed using median filter and morphological bottom-hat filter respectively [9]. In the pre-processed image, morphological gradient operation using circular structuring element has been used to segregate the skin lesion area [9]. In this feature extraction stage, the morphological, texture and color features are quantified for the differentiation of various skin abnormalities. Finally, the skin diseases are classified using an effective classification technique based on those extracted features.

A. Morphological Feature Extraction

From each of the segmented images, structural features including area, perimeter, equivalent diameter, rectangularity, elongation, aspect ratio, solidity, eccentricity, average distance and distance variance have been estimated. For the estimation of the structural abnormality, border irregularity has been calculated from the border detected images. To estimate the border irregularity of the lesion, a border series has been constructed by evaluating the distance of each border pixels from the center pixel. From this border series data, Higuchi fractal dimension (HFD) has been calculated to realize the structural complexity of the skin lesion area [9]. In Fig. 2, the border detected image and corresponding border series have been shown with calculated HFD (HFD=2.8904).

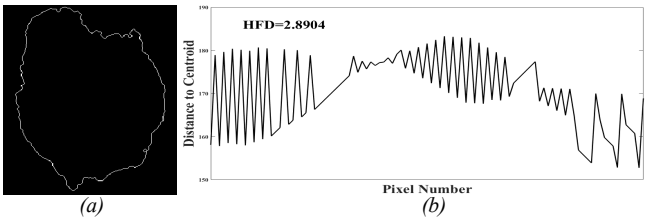

(a) (b)

Fig.2. (a) border detected image; (b) border series and corresponding HFD=2.8904.

B. Empirical Wavelet Transform based Texture Feature Extraction

Among different features, texture feature is the most subjective one which cannot be realised from visual inspection. In this research work, a multi-resolution analysis based texture feature extraction technique is proposed. Empirical wavelet transform (EWT) is introduced as texture feature extracting tool by adaptively selecting the wavelet bases according to the inherent information of the region of interest. The 2D empirical Littlewood-Paley wavelet transform has decomposed the input dermoscopic image in low and high frequency components as explained in Section II. From each of the sub-band images, a fractal descriptor is constructed to estimate the detail textural variation along the lesion area. Fractal dimension estimates the degree of complexity and irregularity in terms of fractional dimension. However, single value fractal dimension is unable to describe the textural complexity sufficiently. Here, empirical wavelet fractal descriptor (EWFD) is introduced by considering the entire fractality curve. From each of the sub band images, fractal descriptor has been constructed to describe the texture complexity of the skin lesion area. For each decomposed images, excluding the zero value coefficients, all the wavelet coefficients are arranged in descending order according to their energy values considering the power law relation. Resultant empirical wavelet fractal descriptor (EWFD) vector is constructed as the following [9]:

$$ED_f : \left\{\left|\log(ED(1))\right|, \left|\log(ED(2))\right|, \cdots, \left|\log(ED(\log_2 m))\right|\right\} \quad (4)$$

Along with EWFD, some statistical features have been extracted as entropy, energy, variance and homogeneity from each of the decomposed components.

C. Color Feature Extraction

To extract the color information from the lesion area, some statistical features have been calculated as minimum, maximum, mean, variance, standard deviation, skewness and entropy.

D. Feature Selection and Classification

After the feature extraction stage, selection of differentiating features is essential for the classification of the diseases with higher identification accuracy. Using the support vector machine recursive feature elimination (SVM-RFE) methodology, important features have been identified

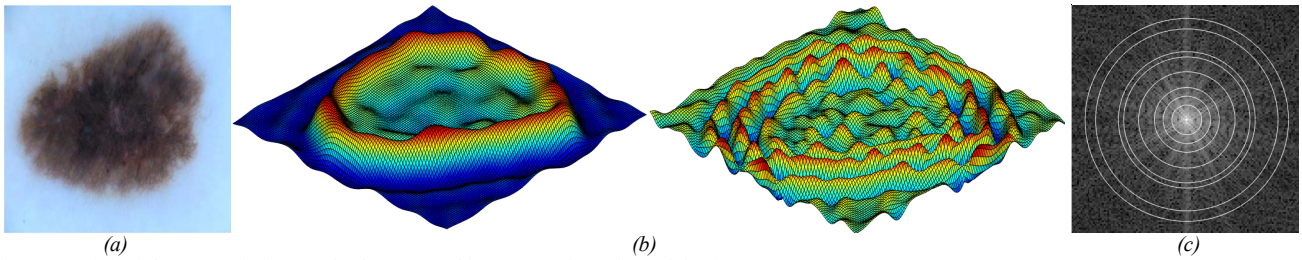

(a) (b) (c)

Fig.2. (a) original dermoscopic image; (b) decomposed images; (c) boundary of the frequency spectrum.

according to their ranking criterion [9]. The entire feature set has been fed to the feature selection algorithm to train a SVM classifier. The entire feature set is arranged according to their estimated weight value. SVM-RFE recursively eliminates the features having smaller ranking criterion. Here, instead of removing a single feature in each iteration, a group of features have been eliminated until number of existing features reaches a chosen threshold value.

After the feature selection stage, a three stage ensemble multi-class classification strategy has been employed for the identification of four skin disease classes: melanoma, nevus, BCC and SK. First stage of the classifier (CLASSIFIER-I) has been used to segregate melanoma from other classes (nevus, BCC and SK). The second stage of the classifier (CLASSIFIER-II) has been introduced to differentiate nevus from the remaining disease classes (BCC and SK). Finally, the last stage of the classifier (CLASSIFIER-III) has identified the BCC and SK skin diseases.

IV. Results and Discussion

A. Dataset Description and Data Preparation

In this research work, four skin disease classes have been considered as melanoma, nevus, BCC and SK. Overall 7,201 dermoscopic images, histopathologically confirmed by expert dermatologist have been considered here. The entire dataset contains 2879 number of melanoma, 3013 of nevus, 796 of BCC and 513 number of SK dermoscopic lesions [10]. To carry out this research work, all the images have been resized to 512 × 512 pixels.

B. Results and Discussion

Here, empirical wavelet transform (EWT) has been implemented to decompose the input image into low and high frequency sub bands. Here, Littlewood Paley decomposition technique is used. To realise the EWT, morphological pre-processing with Gaussian regularization with standard deviation of 0.8 has been chosen. Implementing the pseudo polar Fast Fourier transform, the mean spectrum has been computed for detecting the spectrum boundaries to construct the 2D filter bank. Therefore, EWT has constructed a filter bank according to the information contained in the image under consideration. The EWT has decomposed the input dermoscopic images into low and high frequency sub-bands depending on the number of filters in the filter bank. Example of an dermoscopic image and its corresponding sub-bands have been shown in Fig.2. From Fig.2 it has been realised that the decomposition of the input image in several sub-bands describes the regional textural variations along the skin lesion. To quantify this textural complexity, extraction of statistical features is not sufficient. Construction of fractal descriptor provides a chunk of information to deal with such textural variations. From each of the decomposed images, EWFD has been constructed following the equation 4.

After the feature extraction stage, SVM-RFE feature selection technique is deployed. To implement the feature selection algorithm, the elimination threshold value is selected as 60. Therefore, during the recursive feature elimination, the half of the features have been eliminated according to their ranking criterion at each iteration until the number of existing feature has reached to the value of 60. As the existing features are equal to the elimination threshold value, single feature is eliminated at each iteration until all the features have been ranked according to their weight value.

For the performance analysis of the proposed multi-class classification scheme, three types of kernel functions have been chosen for the linearly non-separable feature set by selecting the associated hyper parameters using grid search based technique. All the three classifiers have been trained with 70% of entire dataset. From Table I, it has been realised that among three non-linear kernel functions, radial basis function (RBF) has identified the four diseases with higher performance indices as 97.53% sensitivity, 96.79% specificity and 96.67% accuracy. SVM classifiers with 2nd order polynomial kernel have classified the diseases with overall accuracy 95.61%. Similarly, 96.19% accuracy has been obtained using 3rd order polynomial kernel.

Considering SVM classifiers with RBF kernel, different set of training and test samples have been selected. The classifiers have been trained with various set of training samples with tenfold cross validation technique. In Table II, classification performance of four disease classes has been determined with 90%, 80%, 70% and 60% of training set. Table II has revealed that training the classifier model with 90% training samples has identified the four disease classes with 98.02% sensitivity, 97.10% specificity and 97.15% accuracy. For 60% training dataset, 96.41% classification accuracy has been estimated. Considering the multi-class classification performance for various set of training and testing samples, an acceptable result has been obtained for 70% training and 30% testing dataset with

TABLE I. Comapartive Study on Different non-linear kernel functions of SVM classifier

Kernel	SN (%)	SP (%)	ACC (%)
RBF	97.53	96.79	96.67
Polynomial (2nd Order)	95.92	95.06	95.61
Polynomial (3rd Order)	96.12	96.31	96.19

TABLE II. Comparative Study for Different Training Set

% Training Data	SN (%)	SP (%)	ACC (%)
90	98.02	97.10	97.15
80	97.66	96.71	96.60
70	97.53	96.79	96.67
60	96.78	96.39	96.41

TABLE III. CLASSIFICATION PERFORMANCE FOR DIFFERENT NUMBER OF FEATURES

Number of Features	SN (%)	SP (%)	ACC (%)
20	98.07	97.31	97.15
30	98.67	98.14	98.31
40	98.73	98.51	98.66
50	98.89	98.81	98.90

ten-fold cross validation technique. Therefore, the performance analysis of the entire research work has been carried out using SVM classifier with RBF kernel with 70% training in ten-fold cross validation technique.

Using the SVM-RFE feature selection technique, important and demarcating features have been identified to improve the classification performance. Various set of features have been selected according to their ranking to use as an input to the classification model. Table III has portrayed the effect of first 20, 30, 40 and 50 features in the multiclass classification of the skin diseases. Table III depicts that based on first twenty selected features the skin disease classes have been identified with 98.07% sensitivity, 97.31% specificity and 97.15% accuracy. The performance indices have been further improved using first thirty and forty features with overall accuracy of 98.31% and 98.66% respectively. Table III shows that as the number of features have been increased performance indices also been improved. However, it is always acceptable to classify the disease with lesser number of features. So, first thirty features have been considered for the classification of the skin diseases. The confusion matrix as shown in Fig.4 is used to validate the performance of the proposed methodology. From the figure, it has been realised that CLASSIFIER I has identified melanoma with 99.20% sensitivity and some of the melanoma images have been misclassified as nevus. CLASSIFIER II has classified nevus with 98.60% sensitivity and misclassified as melanoma and BCC. CLASSIFIER III has differentiated BCC and SK with 98.20% and 98.80% sensitivity respectively.

Table IV enlists a comparative performance analysis of the present methodology with some of the state-of-the-art techniques. 90% sensitivity has been reported by Barata *et. al.* [3] for identifying melanoma. Sensitivity of 90.48%, 82.51%, 82.61% and 80.61% has been achieved by Shimizu *et. al.* [4] for the identification of four disease classes. Jiji *et. al.* [6] have obtained sensitivity of 94% while Xie *et. al.* [11] have reported 95.00% sensitivity for the identification of melanoma. It is clear from table IV that the proposed methodology has outperformed the state-of-the-art techniques for multi-class skin disease diagnosis.

TABLE IV. CLASSIFICATION PERFORMANCE COMPARISON OF PROPOSED METHOD WITH STATE-OF-ART TECHNIQUES

Work	Performance Indices (% SN)
Barata et al. [3]	90.00
Shimizu *et al.*[4]	90.48, 82.51, 82.61, 80.61
Jiji *et. al.*[6]	94.00
Xie *et. al.* [11]	95.00
Chatterjee *et. al* [9]	97.63
Proposed Method	**99.20%, 98.60%, 98.20%, 98.80%**

V. CONCLUSION

This paper reports a methodical approach for the identification of closely similar skin abnormalities as melanoma, nevus, BCC and SK. In this work, empirical wavelet transform is explored to obtain in detail textural variations along the skin lesion. Empirical wavelet fractal descriptor (EWFD) is introduced to quantify the textural complexity of each sub-band images. SVM-RFE feature selection technique is used to select the demarcating features from the entire feature set and classify the diseases with higher degree of accuracy. Using the ensemble multi-class classification strategy, melanoma, nevus, BCC and SK diseases have been identified with 99.20%, 98.60%, 98.20% and 98.80% sensitivity respectively.

Fig.4. Confusion matrix of the classification performance of melanoma, nevus, BCC and SK disease.

ACKNOWLEDGMENT

This work is supported by the Department of Electronics and IT, Govt. of India through 'Visvesvaraya PhD scheme', awarded to Jadavpur University, Kolkata, India.

REFERENCES

[1] J. Serup, G. B. E. Jemec and G. L. Grove, "Handbook of NON-INVASIVEMETHODS and the SKIN," Second Edition, CRC Press, 2006.

[2] H. Pehamberger, M. Binder, A. Steiner and K. Wolff, "In vivo equiluminescencemicroscopy: improvement of early diagnosis of melanoma", J. Invest.Dermatol. vol. 100, pp. 356S–362S, 1993.

[3] C. Barata, M. Ruela, M. Francisco, T. Mendonc and J.S. Marques, "Two systems forthe detection of melanomas in dermoscopic images using texture and color features", IEEE Syst. J. vol. 8, no. 3, pp. 965-979, 2014.

[4] K. Shimizu, H. Iyatomi, M.E. Celebi, K. Norton and M. Tanaka, "Four-Class classcation of skin lesions with task decomposition strategy", IEEE Trans.Biomed. Eng. vol. 62, no. 1, pp. 274-283, 2015.

[5] M. Rastgoo, R. Garcia, O. Morel and F. Marzani, "Automatic di erentiation ofmelanoma from dysplastic nevi", Comput. Med. Imaging Graphics, vol. 43, pp. 44-52, 2015.

[6] G. W. Jiji and P. J. DuraiRajb, "Content-based image retrieval techniques for the analysis of dermatological lesions using particle swarm optimization technique", Appl. Soft Comput., vol. 30, pp. 650-662, 2015.

[7] J. Gilles, "Empirical Wavelet Transform", IEEE Trans on Signal Proc., vol.61, 16, 2013.

[8] J. Gilles, G. Tran and S. Osher, "2D Empirical Transforms. Wavelets, Ridgelets, and Curvelets Revisited", SIAM J. Imgaging Scs., vol.7, no. 1, pp. 157-186.

[9] S. Chatterjee, D. Dey, and S. Munshi, Optimal selection of features using wavelet fractal descriptors and automatic correlation bias reduction for classifying skin lesions, Biomedical Signal Processing and Control, vol. 40, pp. 252-262, 2018.

[10] The International Skin Imaging Collaboration: Melanoma Project.ISIC Archive. [Online]. Available: *https://isic-archive.com.*

[11] F. Xie, H. Fan, Y. Li, Z. Jiang, R. Meng, and A. Bovik, "Melanoma Classification on Dermoscopy Images Using Neural Network Ensemble Model", *IEEE Trans. on Medical Imaging*,vol. 36, no. 3, pp. 849-858, March 2017.